



**HAL**  
open science

## Critical aspects of Raman spectroscopy as a tool for postmortem interval estimation.

Guillaume Falgayrac, Raffaele Vitale, Yann Delannoy, Helene Behal,  
Guillaume Penel, Ludovic Duponchel, Thomas Colard

► **To cite this version:**

Guillaume Falgayrac, Raffaele Vitale, Yann Delannoy, Helene Behal, Guillaume Penel, et al.. Critical aspects of Raman spectroscopy as a tool for postmortem interval estimation.. Talanta Open, 2022, Talanta Open, 249, pp.123589. 10.1016/j.talanta.2022.123589 . hal-04385948

**HAL Id: hal-04385948**

**<https://hal.univ-lille.fr/hal-04385948v1>**

Submitted on 22 Jul 2024

**HAL** is a multi-disciplinary open access archive for the deposit and dissemination of scientific research documents, whether they are published or not. The documents may come from teaching and research institutions in France or abroad, or from public or private research centers.

L'archive ouverte pluridisciplinaire **HAL**, est destinée au dépôt et à la diffusion de documents scientifiques de niveau recherche, publiés ou non, émanant des établissements d'enseignement et de recherche français ou étrangers, des laboratoires publics ou privés.



Distributed under a Creative Commons Attribution - NonCommercial 4.0 International License

1 Critical aspects of Raman spectroscopy as a tool for  
2 postmortem interval estimation

3  
4 Guillaume Falgayrac<sup>1\*</sup>, Raffaele Vitale<sup>2</sup>, Yann Delannoy<sup>1</sup>, H el ene Behal<sup>3</sup>, Guillaume Penel<sup>1</sup>,  
5 Ludovic Duponchel<sup>2</sup>, Thomas Colard<sup>4,5</sup>

6  
7 Affiliations:

8 1 Univ. Lille, CHU Lille, Univ. Littoral C ote d'Opale, ULR 4490 - MABLab- Adiposit  M edullaire  
9 et Os, F-59000 Lille, France

10 2 Univ. Lille, CNRS, UMR 8516 - LASIRE - Laboratoire Avanc e de Spectroscopie pour les  
11 Int eractions la R eactivit  et l'Environnement, F-59000 Lille, France

12 3 Univ. Lille, CHU Lille, ULR 2694 - METRICS:  valuation des technologies de sant  et des  
13 pratiques m edicales, F-59000 Lille, France

14 4 Univ. Bordeaux, CNRS, MCC, PACEA, UMR 5199, F-33600 Pessac, France.

15 5 Department of Oral Radiology, University of Lille, Lille University Hospital, F-59000 Lille,  
16 France.

17  
18 \*Corresponding author: [guillaume.falgayrac@univ-lille.fr](mailto:guillaume.falgayrac@univ-lille.fr)

19 Guillaume FALGAYRAC

20 MABLab ULR4490

21 Faculty of Dentistry

22 Place de Verdun

23 59000 Lille FRANCE

24  
25 Keywords: Raman spectroscopy, chemometrics, forensics, bone, ANOVA-simultaneous  
26 component analysis, burial

27

28

29

30        **Abstract**

31            The estimation of the postmortem interval (PMI) from skeletal remains represents a  
32 challenging task in forensic science. PMI is often influenced by extrinsic factors (humidity, dry,  
33 scavengers, etc.) and intrinsic factors (age, sex, pathology, way of life, medical treatments,  
34 etc.). Raman spectroscopy combined with multivariate data analysis represents a promising  
35 tool for forensic anthropologists. Despite all the advantages of the technique, Raman spectra  
36 of skeletal remains are influenced by these extrinsic and intrinsic factors, which impairs  
37 precision and reproducibility. Both parameters have to reach a high level of confidence when  
38 such spectroscopy is used as a way to predict PMI. As a consequence, advanced multivariate  
39 data analysis is necessary to quantify the effect of all factors to improve the estimation of the  
40 PMI.

41            The objective of this work is to evaluate the effect of intrinsic and extrinsic factors on  
42 the Raman spectra of skeletal remains. We designed a protocol close to a real-world scenario.  
43 We used ANOVA-simultaneous component analysis (ASCA) to unmix and quantify the effect  
44 of 1 intrinsic (source body) and 1 extrinsic (burial time) factors on the Raman spectra. In our  
45 model, the burial time (15.66%) was found to generate the highest variability after the source  
46 body (7.54%). ASCA showed that the variability due to the burial time has 2 mixed  
47 contributions. Seasonal variations are the first contribution. The second contribution is  
48 attributed to diagenesis. A decrease in the mineral band and an increase in the organic bands  
49 are observed. The source body was also found to contribute to the variability in Raman  
50 spectra. ASCA showed that the source body induces variability related to the composition of  
51 bone. This quantification cannot be assessed by basic chemometrics methods such as PCA.  
52 The results of this study highlighted the need to use an advanced chemometric data analysis  
53 tool (ASCA) combined with Raman spectroscopy to estimate the postmortem interval.

54

## 55 1 INTRODUCTION

56 Upon discovering skeletal remains, forensic anthropologists must answer several  
57 questions. These include determining the cause of death, identifying the deceased, and  
58 determining the postmortem interval (PMI). PMI corresponds to the delay between death and  
59 the discovery of the body. Thus, its estimation is a crucial part of forensic investigation.  
60 Beyond a certain PMI (which varies from country to country), a criminal investigation cannot  
61 be pursued. In France, the threshold is set at 20 years. Even if this estimation is a crucial step,  
62 forensic investigators do not have access to reliable and accurate methods at this time. Bell et  
63 al. called to strengthen the effort of scientific researchers and forensic doctors to improve  
64 forensic methods [1].

65 The estimation of the PMI from skeletal remains represents a challenging task in forensic  
66 medicine [2]. The PMI is often influenced by extrinsic factors (humidity, dry, scavengers, etc.)  
67 and intrinsic factors (age, sex, pathology, way of life, medical treatments, etc.). The existing  
68 methods involve the study of reactive molecules between bone and substrates [3-5],  
69 measurement of bone radioisotopes [6], and other physicochemical techniques [7-9]. Among  
70 these, vibrational spectroscopy (and particularly Raman spectroscopy) was found to yield  
71 satisfactory results in diverse application scenarios: it enabled the discrimination of forensic  
72 and archaeological remains [10], the differentiation of human and nonhuman bones [11], and  
73 the effect of diagenesis on bone molecular composition [12]. From these few examples,  
74 Raman spectroscopy represents a promising tool for forensic scientists with serious  
75 advantages. First, this spectroscopic analysis can be performed on a sample without  
76 preparation (or a few simple steps). Second, the technique simultaneously provides molecular  
77 information on the mineral and organic compounds in the bone. The last advantage is the  
78 nondestructive character of this analysis method. Indeed, the possibility of analyzing samples  
79 while preserving them is a real leitmotiv in forensic medicine. Handheld Raman spectroscopy  
80 devices are currently largely available on the market and constitute important resources for  
81 forensic investigators since they enable direct on-field operations [13].

82 Despite all the aforementioned pros, the global information encoded in a Raman  
83 spectrum can be considerably influenced by multiple factors at the same time, which often  
84 leads to scarce precision and reproducibility in the estimation of PMI values. Wang *et al.*  
85 highlighted this limitation in their study on human bone [2]. Creagh *et al.* used an animal

86 model to minimize these variations [14]. Mc Laughlin *et al.* stressed the need for advanced  
87 statistical methods for modeling the multiple sources of variation affecting vibrational  
88 spectroscopy data of bone samples [15]. Recent works considered the effect of intrinsic and  
89 seasonal factors in their approach but without the possibility of quantifying them from the  
90 data [16, 17]. More importantly, all attempts to use basic chemometric techniques such as  
91 principal component analysis (PCA) or partial least squares (PLS) regression without explicitly  
92 accounting for the effect of such factors resulted in suboptimal solutions [18].

93 In other scientific fields, such as metabolomics and food science, chemometricians  
94 have addressed the problem of disentangling these different sources of variation using an  
95 original multivariate data analysis approach called ANOVA-simultaneous component analysis  
96 (ASCA). ASCA combines the principles of both design of experiments (DoE) and multivariate  
97 exploratory analysis to evaluate whether a set of acquired data is significantly affected by  
98 specific experimental parameters (and/or interactions between them) and potentially  
99 quantify their effect on the measurements [19].

100 The objective of this work is to evaluate the effect of 1 intrinsic (source body) and 1  
101 extrinsic factor (burial time) on the Raman spectra of skeletal remains. We designed an  
102 analytical protocol so as to get as close as possible to the real-world conditions observed  
103 during such a characterization. Then, the ASCA method was used to quantify the effect of the  
104 2 factors and their interaction on the acquired Raman spectra.

## 105 2 MATERIAL AND METHODS

### 106 2.1 Samples

107 Six human subjects without known bone pathology were considered in this work (Table  
108 1). All subjects were Caucasian and died of a heart attack. To comply with ethical standards,  
109 the analyzed bones were obtained from individuals who had "donated their bodies to science"  
110 according to a specific French law, which allows anatomic dissections and research to be  
111 performed on these human cadavers. Ribs were chosen for investigation given their  
112 importance in anthropology (e.g., estimating the age at death) [20, 21]. It was decided to work  
113 with fresh bone samples as embalming procedures induce changes in their molecular  
114 composition [22]. Moreover, the use of fresh ribs permits mimicking the conditions of a real-  
115 case scenario of discovery of skeletal remains.

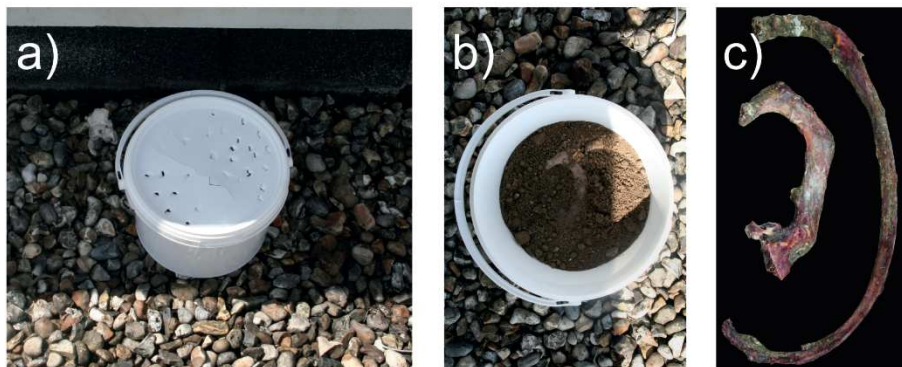
116

117 **Table 1: Characteristics of the subjects: 4 males and 2 females. Mean age of the group: 83.5 ( $\pm$  7.1) year-old.**

ID	Gender	Age	observations
#1	male	72	no records
#2	female	92	coxarthrosis, knee surgery, osteonecrosis of the femoral head
#3	female	80	heart prosthetic stent, vascular issues, Alzheimer's disease
#4	male	88	hypertension
#5	male	82	acute myeloid leukemia, alcoholism, smoker
#6	male	87	no records

118

119 The experimental protocol was designed as follows. For each subject, two ribs (R1 and R4)  
120 were harvested on the day of death. The flesh surrounding bones was mechanically removed  
121 without any further treatment. A 5-mm-long section of bone was cut transversally across each  
122 rib using a diamond saw. The bone section was then used for Raman microscopy. These  
123 samples represented the baseline (T0). The holes resulting from this preparatory step were  
124 then covered with neutral wax before the ribs were placed back in their burial environment.  
125 The latter procedure was repeated each month for 12 months. Each pair of ribs (R1 and R4)  
126 from the same subject was placed into its own tray (Figure 1a). Each plastic tray was filled with  
127 clay soil typical of northern France. The soil pH was 6.8 and described as brown to brown  
128 leached, low hydromorphic, aeolian silt on clay and sandy substrate of the Lille Region (Table  
129 2). The ribs were covered by approximately 1 cm of soil (Figure 1b). Plastic trays were placed  
130 outside and under cover to protect them from scavengers and rain. This sampling method has  
131 been shown not to induce any change in the sample [23]. The local weather data were  
132 retrieved from the Météo France website (Table 2).



133

134 *Figure 1: a) plastic tray with lid to protect from scavengers. The plastic tray was sheltered to protect from rain;*  
 135 *b) plastic tray filled with clay soil typical of northern France carrying the rib; c) ribs n°1 and 4 after 1 month of*  
 136 *burial time*

137 *Table 2: Features of the burial environments of the first and fourth ribs (labeled R1 and R4, respectively). For*  
 138 *each subject, R1 and R4 ribs were placed on a soil surface and covered by an approximately 1 cm thin layer of*  
 139 *soil.*

<b>R1 and R4</b>	
<b>Bone class</b>	First and fourth right ribs
<b>Environment</b>	Outdoor
<b>Environmental conditions</b>	Under cover
<b>Soil type/pH</b>	Clay/6.8
<b>Temperature range during the experiment (mean ±SD) in °C</b>	T° mean: 10.5 ±4.7 T°max: 14.4 ±5.4 T°min: 7.0 ±4.2
<b>Relative humidity (%)</b>	79.5 ±6.8

140

## 141 2.2 Raman microspectrometry

142 Each 5-mm-long section of ribs was analyzed by Raman microspectroscopy every month for  
 143 one year. The spectrometer was installed in a room with controlled temperature. Raman  
 144 spectra were acquired with a LabRAM HR800 Raman microspectrometer (Jobin-Yvon,  
 145 Villeneuve d'Ascq, France) equipped with DuoScan technology, an XYZ motorized stage, and a  
 146 785 nm laser diode [24]. A mean spectrum was acquired over a rastered bone area of 30 x 30  
 147  $\mu\text{m}^2$ . The acquisition time was set to 30 s, considering a 300-1700  $\text{cm}^{-1}$  spectral domain. Prior  
 148 to spectroscopic acquisition, each 5-mm-long section was stuck on a microscope slide and  
 149 polished with decreasing grain size (from 30 to 0.3  $\mu\text{m}$ ). For each rib, 4 specific zones were  
 150 anatomically identified: secondary osteon, interstitial bone, periosteum, and trabecular bone.  
 151 Ten spectra were acquired per anatomic zone, ultimately resulting in 40 spectra per rib per  
 152 month. The 2 final sets of 40 spectral profiles per rib per month (max-normalized) were joint  
 153 and averaged prior to further processing.

## 154 2.3 The proposed multivariate approach: ANOVA-simultaneous component analysis 155 (ASCA)

156 ANOVA-simultaneous component analysis (ASCA) combines the advantages of both design of  
 157 experiments and multivariate exploratory analysis to study whether the recorded data are

158 significantly affected by certain experimental parameters or factors (and/or by the interaction  
 159 of multiple factors) and to assess how they actually vary under their influence [25, 26]. Let  $\mathbf{X}$   
 160 be a two-dimensional data structure whose rows correspond to the Raman spectra collected  
 161 and whose columns to the spectral channels sampled. Mathematically speaking, ASCA  
 162 decomposes the centered data matrix ( $\bar{\mathbf{X}}$ ) into the sum of several arrays according to the  
 163 ANOVA scheme. In this work, the effects of the source body (Factor A) and the burial time  
 164 (Factor B) on the evolution of the bone composition will be investigated. The partition of  $\bar{\mathbf{X}}$  is  
 165 carried out as:

$$\bar{\mathbf{X}} = \mathbf{X}_A + \mathbf{X}_B + \mathbf{X}_{AB} + \mathbf{E} \quad (1)$$

166  
 167 where  $\mathbf{X}_A$ ,  $\mathbf{X}_B$  and  $\mathbf{X}_{AB}$  account for the variability induced by the effect of Factor A, Factor B  
 168 and Factor A/Factor B interaction, respectively, while  $\mathbf{E}$  carries the residuals not explained by  
 169 the model.

170 To evaluate whether the effect of a factor/interaction on the data variation is statistically  
 171 significant, the sum-of-squares of the corresponding submatrix is computed as in Eq. 2:

$$SSQ_i = \|\mathbf{X}_i\|^2 \quad \forall i = \{A, B, AB\} \quad (2)$$

172  
 173 with  $\|\cdot\|^2$  denoting the Euclidean norm.  $SSQ_i$  is afterward contrasted against a *null*  
 174 distribution nonparametrically estimated by permutation testing conducted on the residuals  
 175 of the so-called *reduced model* (i.e., by shuffling the rows of the augmented matrix obtained  
 176 by summing the sub-array related to the specific factor or interaction under study and  $\mathbf{E}$ ) [27,  
 177 28]. If the observed sum-of-squares is found to be systematically larger than the values of such  
 178 a *null* distribution ( $p \text{ value} < 0.05$ ), the tested effect is then assumed to be statistically  
 179 significant and  $\mathbf{X}_i$  decomposed by simultaneous component analysis (SCA) as:

$$\mathbf{X}_i = \mathbf{T}_i \mathbf{P}_i^T \quad (3)$$

181  
 182 where  $\mathbf{T}_i$  and  $\mathbf{P}_i$  are the scores and the loadings matrices resulting from a principal  
 183 component analysis (PCA) model constructed under the ANOVA scheme constraint. The  
 184 graphical representation of  $\mathbf{T}_i$  and  $\mathbf{P}_i$  provides direct insights into the data variability induced  
 185 by the concerned factor/interaction.

186 From a technical perspective, according to the theory of design of experiments, factor A and  
187 factor B have a different inherent nature: the former is defined as random, while factor B can  
188 be considered as fixed. In principle, random factors cannot be readily coped with by the  
189 classical implementation of ASCA, which is capable of directly handling only fixed ones.  
190 Nonetheless, in statistics, it is rather common to fit random factors as fixed especially when  
191 the amount of levels spanned (here, the number of source bodies) is limited or the  
192 distributional assumptions that need to be fulfilled for modelling random factors as such do  
193 not necessarily hold (this happens, for example, if they are associated to relatively strong  
194 effects and/or their levels are not drawn from a homogeneous population, as is to be expected  
195 in this particular case-study) [29, 30]. For this reason, for the sake of simplicity and in the light  
196 of the fact that virtually identical results were obtained by means of an alternative approach  
197 that preserves the *randomness* of factor B (*i.e.*, repeated measures ASCA+ [31] – not shown),  
198 only the outcomes returned by standard ASCA will be discussed in the following sections.

## 199 3 Results

### 200 3.1 The extrinsic and intrinsic factors have a significant contribution to the data 201 variability

202 A classical PCA was applied to the original spectral dataset, but no clear separation of  
203 the samples according to their corresponding burial time was found (data not shown). This is  
204 representative of the presence of multiple sources of variation (intrinsic and extrinsic factors)  
205 simultaneously affecting the data and potentially masking those of interest [11, 18]. ASCA was  
206 applied to take into account the effect of these factors. One intrinsic and one extrinsic factors  
207 were considered: the subject (from 1 to 6) and the burial time (from baseline to 12 months).  
208 These factors were modeled separately to quantify their effect on the Raman spectra.  
209 Permutation tests were exploited to test the effect of these two factors and their binary  
210 interaction on the variation of the collected Raman spectra. Table 3 summarizes the results  
211 obtained after 1000 permutations.

212

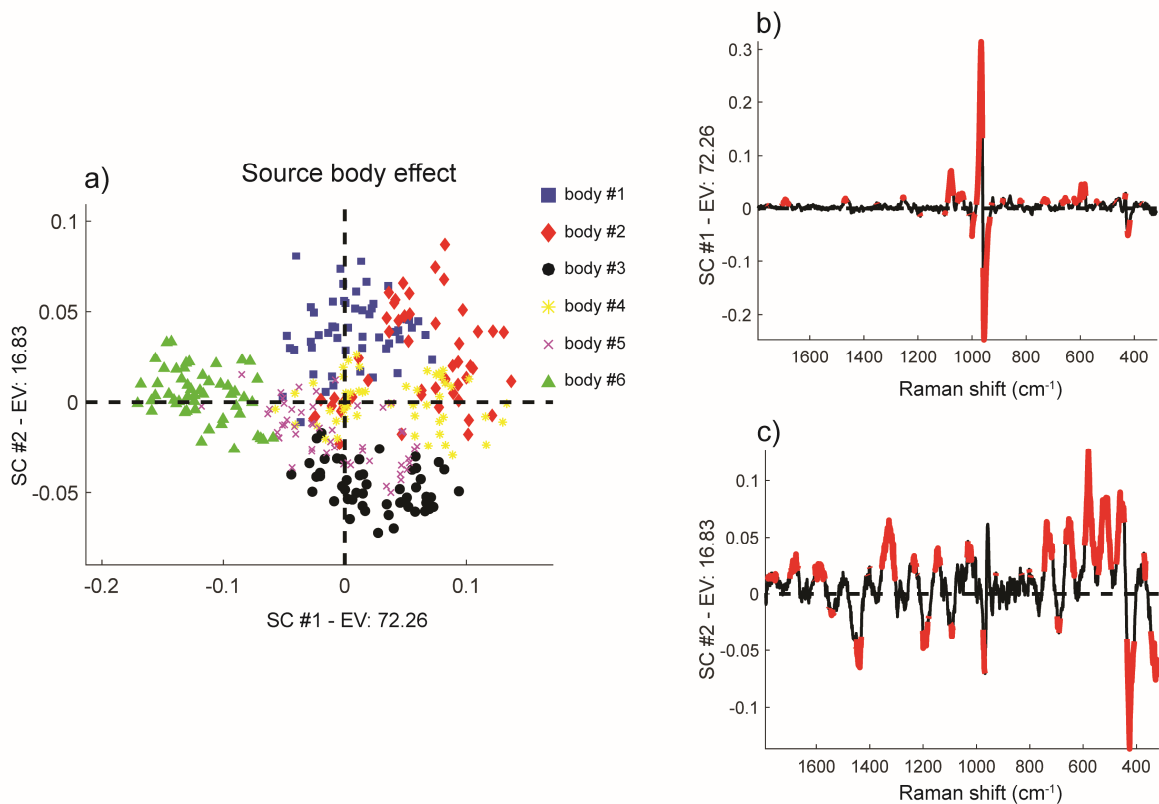
213 **Table 3: Summary of the ASCA results. The percentage of variance explained is calculated with respect to the**  
 214 **mean-centered data,  $\bar{X}$ . Results obtained after 1000 permutations.**

Factor/interaction	Factor/interaction array	<i>p</i> value	Variance explained (%)
Source body	$\mathbf{X}_A$	<0.001	7.54%
Burial time	$\mathbf{X}_B$	<0.001	15.66%
Source body/burial Time	$\mathbf{X}_{AB}$	<0.001	56.79%

215  
 216 The two main factors (*i.e.*, source body and burial time) as well as the binary interaction source  
 217 body/burial time were found to have a statistically significant influence on the recorded  
 218 measurements.  $\mathbf{X}_A$ ,  $\mathbf{X}_B$  and  $\mathbf{X}_{AB}$  were therefore decomposed as in Equation 3 for a visual  
 219 inspection of such induced changes. More specifically, to better differentiate the samples  
 220 characterized at the distinct levels of each factor/interaction, SCA scores accounting for  
 221 within-level variability were estimated as [32]:

$$\mathbf{T}_{(\mathbf{X}_i + \mathbf{E})} = (\mathbf{X}_i + \mathbf{E})\mathbf{P}_i \quad (4)$$

222  
 223  
 224 In addition, to enable a more straightforward interpretation of the final ASCA model, the  
 225 corresponding loadings were subjected to a statistical bootstrapping procedure that  
 226 permitted to readily identify the spectral features mainly responsible for the observed  
 227 differences [31, 33-35]. This procedure encompasses two sequential algorithmic steps  
 228 (iterated 1000 times): first, bootstrapping with substitution is carried out on a random number  
 229 of raw spectral profiles within each individual level of the simple factors or binary interaction  
 230 under study. Afterwards, the resulting data matrix is decomposed according to the same ASCA  
 231 model built on the original one. It is important to notice here that, as slightly different versions  
 232 of the initial data array are repeatedly analyzed, the ASCA loadings retrieved at each  
 233 bootstrapping iteration need to be rotated with respect to some common reference profiles.  
 234 In this particular case, such loadings were orthogonal Procrustes-rotated towards those  
 235 extracted from the non-bootstrapped data.



236

237 Figure 2 represents the outcomes yielded by the decomposition of  $\mathbf{X}_A$  (source body effect)<sup>1</sup>.

238 Scores clearly clustered according to the source body index along the first and second

239 simultaneous components (SCs) (Figure 2a). The SC#1 loadings are characterized by an intense

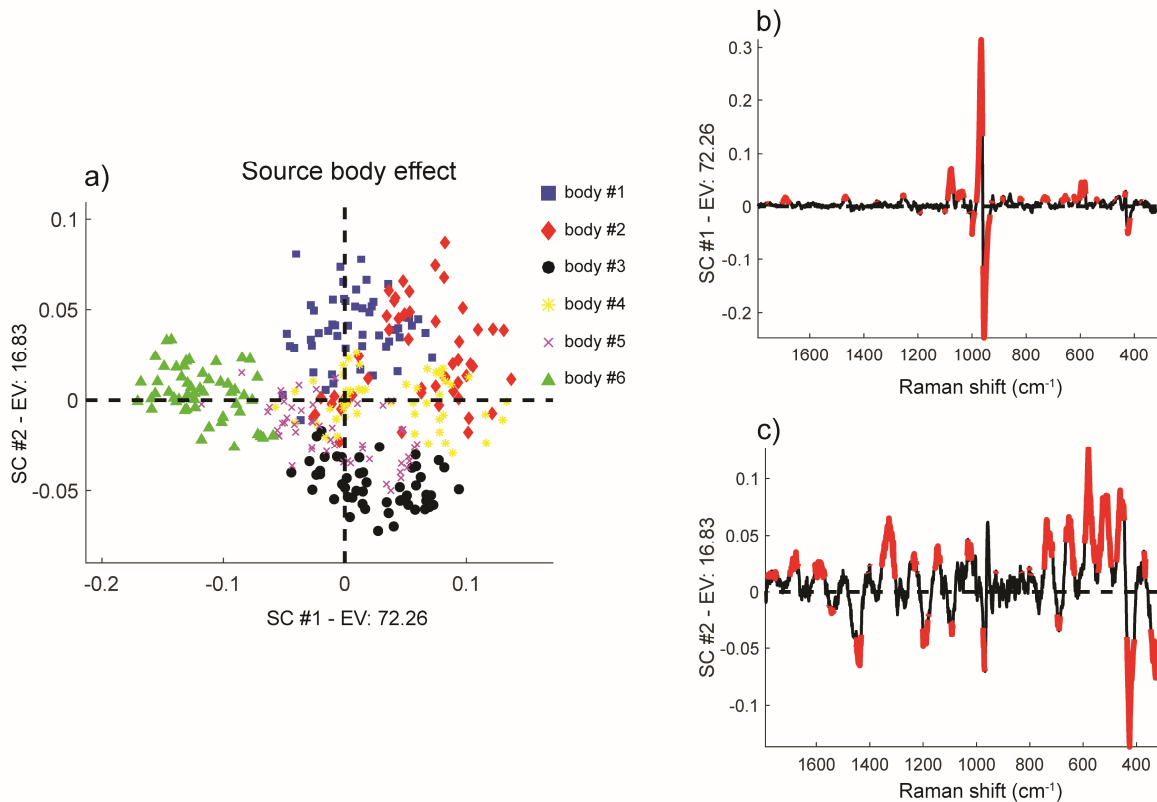
240 band at 960  $\text{cm}^{-1}$  assigned to phosphate vibration ( $\nu_1\text{PO}_4$ ) and a minor band at 1070  $\text{cm}^{-1}$

241 assigned to carbonate vibration ( $\nu_1\text{CO}_3$ ). The SC#2 loadings are characterized by Raman bands

242 assigned to the organic and mineral matrix: 1670  $\text{cm}^{-1}$  (amide I), 1450  $\text{cm}^{-1}$  ( $\text{CH}_2$  collagen type

243 I), 1260  $\text{cm}^{-1}$  (amide III), 590  $\text{cm}^{-1}$  ( $\nu_4\text{PO}_4$ ) and 430  $\text{cm}^{-1}$  ( $\nu_2\text{PO}_4$ ).

<sup>1</sup> For every factor/interaction effect matrix, the lowest number of components explaining approximately 90% of its variance was extracted.

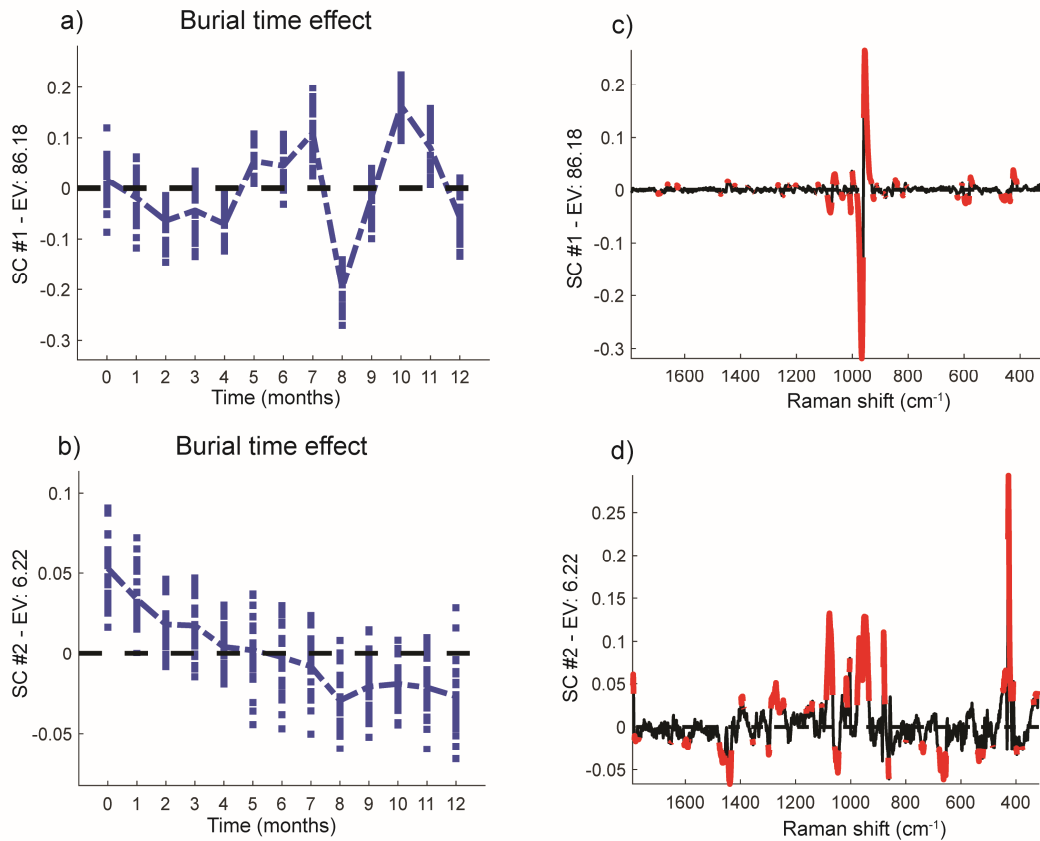


244

245 **Figure 2: a)  $X_A$  SC1 vs. SC2 scores plot. Legend: body #1 (blue squares); body #2 (red diamonds); body #3 (black**  
 246 **circles); body #4 (yellow stars); body #5 (magenta crosses); body #6 (green triangles).  $X_A$  loadings profiles**  
 247 **along b) SC1 and c) SC2. Loading values found to be either always positive or always negative across 1000**  
 248 **bootstrapping iterations and, therefore, associated with wavelength channels relevant for the sake of**  
 249 **interpretation are highlighted in red. SC and EV stand for simultaneous component and explained variance,**  
 250 **respectively.**

251

252 Figure 3 shows the output of the ASCA analysis for  $X_B$  (burial time). The scores along SC#1  
 253 (Figure 3a) follow a sinusoidal temporal trend. The outlying behavior noticeable at months 8  
 254 and 9 is due to a power failure of the laser, which was replaced at month 10. The SC#1 loadings  
 255 are characterized by a strong contribution at 960 cm<sup>-1</sup>. The scores along SC#2 decrease  
 256 continuously as a function of burial time. Positive scores are observed for spectra collected  
 257 between 0 and 5 months, and negative scores are observed for spectra collected between 5  
 258 and 12 months. Positive and negative loadings are found for mineral and organic bands,  
 259 respectively.



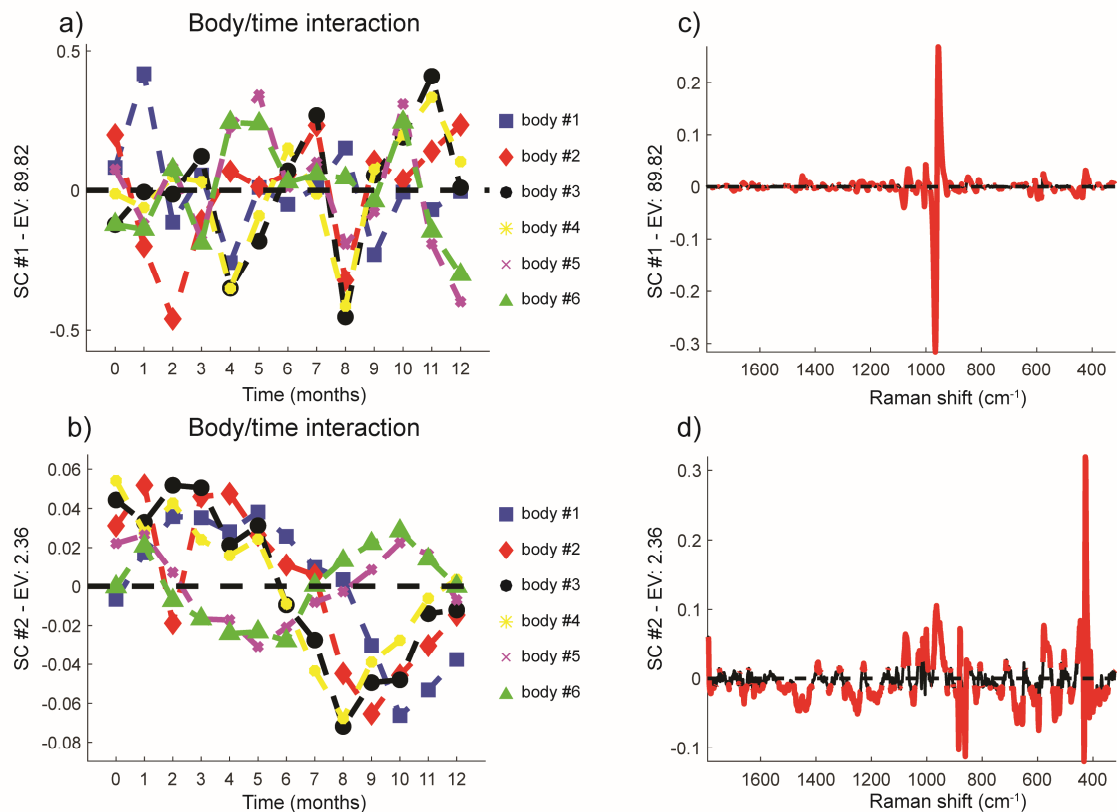
260

261 **Figure 3: Longitudinal plots of the a) first and b) second  $X_B$  SC scores. Here, each sample at each month is**  
 262 **represented as a blue square. The dashed line connects the mean scores values calculated at the different time**  
 263 **steps.  $X_B$  loadings profiles along c) SC1 and d) SC2. Loading values found to be either always positive or always**  
 264 **negative across 1000 bootstrapping iterations and, therefore, associated with wavelength channels relevant**  
 265 **for the sake of interpretation are highlighted in red. SC and EV stand for simultaneous component and**  
 266 **explained variance, respectively.**

267

### 268 3.2 The interaction “PMI+body/PMI” interactions

269 In the last step and as recommended in previous works, SCA was performed on  $(X_B + X_{AB})$   
 270 to more systematically explore the effect of the binary interaction source body/burial time  
 271 [34, 35]. In this regard, both the SC#1 and SC#2 longitudinal scores plots in Figure 4a and 4b  
 272 show profiles fluctuating (with different frequencies) and substantially shifting in time for the  
 273 concerned six source bodies. The largest contributions to these two components are given by  
 274 the Raman band centered at  $960\text{ cm}^{-1}$  and by the mineral and organic bands attributed  
 275 beforehand, respectively.



276  
 277 **Figure 4: Longitudinal plots of the a) first and b) second ( $X_B + X_{AB}$ ) SC scores. Here, each sample at each burial**  
 278 **time point is represented as a symbol of a different color; body #1 (blue squares); body #2 (red diamonds);**  
 279 **body #3 (black circles); body #4 (yellow stars); body #5 (magenta crosses); body #6 (green triangles). The**  
 280 **dashed lines connect the mean scores values calculated at the different time steps for each source body (line**  
 281 **colors are coherent with those of the corresponding symbols). ( $X_B + X_{AB}$ ) loadings profiles along c) SC1 and**  
 282 **SC2. Loading values found to be either always positive or always negative across 1000 bootstrapping**  
 283 **iterations and, therefore, associated with wavelength channels relevant for the sake of interpretation are**  
 284 **highlighted in red. SC and EV stand for simultaneous component and explained variance, respectively.**

## 285 4 Discussion

286 In the last 5 years, various studies have been published to establish a proof-of-concept  
 287 about the use of vibrational spectroscopy to analyze bones in the forensic field. Each study  
 288 addresses specific questions: comparison of techniques of analysis [36, 37]; comparison of  
 289 chemometric methods [2]; differentiation of archeologic vs forensic bones [10]; diagenesis of  
 290 burned bones [38]; estimation of the PMI [16]; and use of animal bones as a human proxy  
 291 [11]. Most of the studies used infrared spectroscopy (FTIRM, IR reflexion, ATR, or MIR) to a  
 292 much lesser extent than Raman microspectroscopy. All studies agree that vibrational  
 293 techniques are suitable for forensic investigation. However, there are still issues to overcome  
 294 to make vibrational techniques ready-to-use for forensic investigators. One recurrence is the  
 295 influence of intrinsic and extrinsic factors on the infrared and Raman spectra of bones. This

296 issue, commonly highlighted in previous studies, impairs precision and reproducibility [2, 14-  
297 16, 18]. These studies employed chemometric techniques such as principal component  
298 analysis (PCA), partial least square (PLS) regression, or genetic algorithms. The precision and  
299 reproducibility were improved by the chemometric approach compared to univariate analysis.  
300 PCA is commonly used to highlight spectral differences between datasets from 2 specific  
301 conditions. PCA revealed differences between groups when one condition was tested and  
302 other factors remained equivalent. However, in the situation of a follow-up of degradation of  
303 bones in their environment, there are extrinsic and intrinsic factors that represent different  
304 sources of spectral variation. PCA is not able to make the difference between all the sources  
305 of variations as it does not directly account for their effect, which resulted in a limited  
306 improvement.

307       Based on these observations, the objective of this study was to critically evaluate Raman  
308 spectroscopy as a tool for estimating the burial time by considering the effect of one intrinsic  
309 and one extrinsic factor. We designed a protocol close to a real-world scenario. We used an  
310 advanced multivariate method (ASCA) to separate and quantify the effects of these factors  
311 (body and burial time) on the Raman spectra. We quantified these effects on the variability of  
312 the considered dataset. In our model, the effect was ranked as follows: burial time (15.66%)  
313 > source body (7.54%).

314       The first factor, “burial time” (extrinsic factor), represents the highest variability,  
315 explaining 15.66% compared to the other. Among these 15.66%, the ASCA analysis revealed 2  
316 contributions. The scores of SC#1 follow a sinusoidal trend within 12 months of burial time  
317 and represent 86.18% of the variance explained. This sinusoidal trend is likely caused by yearly  
318 seasonal fluctuations even in a room with controlled temperature. This result suggests that  
319 yearly variations might not be related to room temperature but to another factor that is  
320 difficult to identify with this protocol. The scores of SC#2 follow a decreasing trend within 12  
321 months of burial time and represent 6.22% of the variance explained. SC#2 accounts for a  
322 decrease in the Raman intensity of the mineral bands and an increase in the Raman intensity  
323 of the organic bands over burial time. The decrease in mineral bands and the increase in  
324 organic bands suggest a decrease in the mineral/organic ratio parameter. This parameter was  
325 also found to decrease when the burial period was less than 24 months in an animal model  
326 [14, 15]. The use of advanced chemometrics methods is strongly recommended in the light of

327 these results. The low contribution of the burial time to the variability could explain the  
328 absence of clustering on the PCA results.

329 The intrinsic factor considered was the source body which accounted for 7.54% of the  
330 total variability observed. Among the 7.54%, ASCA detected 2 main contributions. SC#1  
331 (72.26%) relates to mineral bands, and SC#2 (16.83%) to organic bands. These results indicate  
332 that bone samples show characteristic spectroscopic signatures depending on the subject;  
333 therefore, the bone composition varies among subjects. Such a variation is related to  
334 interindividual differences and may have multiple origins: gender [39], age [40, 41], drugs [42],  
335 pathologies [43], food intake [44], and so on. Therefore, with the aim of using Raman  
336 spectroscopy as a tool for estimating the burial time, the variability associated with the  
337 subject's history should be taken into account. In our model, it accounts for 7.54% of the  
338 explained variance (half of the effect of the burial time). It represents anyway a significant  
339 source of variation which can lead to an error in the estimation of the burial time.

340 This study has limitations related to the investigation of human samples. First, the study  
341 was performed with a limited number of subjects (n=6). The number of samples was limited  
342 due to the accessibility of fresh human samples. The authors excluded bone samples that were  
343 fixed by any protocol because it modifies the composition of bone [22, 45]. Second, bone  
344 samples were obtained from old subjects. The inclusion of younger subjects would have been  
345 a serious constraint within the timeframe of the study.

## 346 5 Conclusion

347 The objective of this work was to evaluate the effect of environmental factors on the  
348 Raman spectra of skeletal remains. The effect of two factors (source body and burial time) and  
349 their binary interaction on the variability of the spectral profiles was quantified and assessed.  
350 Our approach provides a clear overview of how Raman bands evolve under the action of every  
351 single factor/interaction. In our experimental design, the burial time and the source body had  
352 a significant contribution to the variability of the collected data. From a forensic point of view,  
353 the results of this study show that (i) an advanced chemometric data analysis tool (ASCA) is  
354 needed when attempting to use Raman spectroscopy for the estimation of PMI and (ii) the  
355 intrinsic factor "source body" may alter the estimation of the PMI.

356

357 6 Authors contribution

358 Y.D., T.C., G.F., G.P. designed the research. Y.D., G.F. performed research. Y.D acquired data.  
359 L.D., R.V., H.B. performed the statistical analysis. Y.D., T.C., G.F, G.P., L.D., R.V. interpreted the  
360 data. Y.D., T.C., G.F, L.D., R.V. wrote the paper. All authors read and approved the paper.

## 361 7 Acknowledgements

362 The authors thanks Olivier Devos for his precious advices at the beginning of the study.

## 363 8 References

- 364 [1] S. Bell, S. Sah, T.D. Albright, S.J. Gates, Jr., M.B. Denton, A. Casadevall, A call for more  
365 science in forensic science, *Proc. Natl. Acad. Sci. U. S. A.* 115(18) (2018) 4541-4544.
- 366 [2] Q. Wang, Y. Zhang, H. Lin, S. Zha, R. Fang, X. Wei, S. Fan, Z. Wang, Estimation of the late  
367 postmortem interval using FTIR spectroscopy and chemometrics in human skeletal remains,  
368 *Forensic Sci. Int.* 281 (2017) 113-120.
- 369 [3] S. Berg, The determination of bone age, *Methods of forensic science*, vol. 21963, pp. 231-  
370 252.
- 371 [4] F. Ramsthaler, S.C. Ebach, C.G. Birngruber, M.A. Verhoff, Postmortem interval of skeletal  
372 remains through the detection of intraosseal hemin traces. A comparison of UV-fluorescence,  
373 luminol, Hexagon-OBTI(R), and Combur(R) tests, *Forensic Sci. Int.* 209(1-3) (2011) 59-63.
- 374 [5] J.M. Very, R. Gibert, B. Guilhot, M. Debout, C. Alexandre, Effect of aging on the amide group  
375 of bone matrix, measured by FTIR spectrophotometry, in adult subjects deceased as a result  
376 of violent death, *Calcif. Tissue Int.* 60(3) (1997) 271-5.
- 377 [6] B. Swift, I. Lauder, S. Black, J. Norris, An estimation of the post-mortem interval in human  
378 skeletal remains: a radionuclide and trace element approach, *Forensic Sci. Int.* 117(1-2) (2001)  
379 73-87.
- 380 [7] M.A. Brown, A.W. Bunch, C. Froome, R. Gerling, S. Hennessy, J. Ellison, Citrate Content of  
381 Bone as a Measure of Postmortem Interval: An External Validation Study, *J. Forensic Sci.* 63(5)  
382 (2018) 1479-1485.
- 383 [8] M.A. Castellano, E.C. Villanueva, R. von Frenckel, Estimating the date of bone remains: a  
384 multivariate study, *J. Forensic Sci.* 29(2) (1984) 527-34.
- 385 [9] K. Johnsson, Chemical Dating of Bones Based on Diagenetic Changes in Bone Apatite,  
386 *Journal of Archaeological Science* 24 (1997) 431-437.
- 387 [10] T. Leskovar, I. Zupanic Pajnic, I. Jerman, M. Cresnar, Separating forensic, WWII, and  
388 archaeological human skeletal remains using ATR-FTIR spectra, *Int. J. Legal Med.* (2019).
- 389 [11] Q. Wang, W. Li, R. Liu, K. Zhang, H. Zhang, S. Fan, Z. Wang, Human and non-human bone  
390 identification using FTIR spectroscopy, *Int. J. Legal Med.* 133(1) (2019) 269-276.
- 391 [12] G. Dal Sasso, I. Angelini, L. Maritan, G. Artioli, Raman hyperspectral imaging as an effective  
392 and highly informative tool to study the diagenetic alteration of fossil bones, *Talanta* 179  
393 (2018) 167-176.
- 394 [13] W.R. de Araujo, T.M.G. Cardoso, R.G. da Rocha, M.H.P. Santana, R.A.A. Munoz, E.M.  
395 Richter, T. Paixao, W.K.T. Coltro, Portable analytical platforms for forensic chemistry: A review,  
396 *Anal. Chim. Acta* 1034 (2018) 1-21.
- 397 [14] D. Creagh, A. Cameron, Estimating the Post-Mortem Interval of skeletonized remains: The  
398 use of Infrared spectroscopy and Raman spectro-microscopy, *Radiat Phys Chem* 137 (2017)  
399 225-229.
- 400 [15] G. McLaughlin, I.K. Lednev, Potential application of Raman spectroscopy for determining  
401 burial duration of skeletal remains, *Anal. Bioanal. Chem.* 401(8) (2011) 2511-8.
- 402 [16] A. Baptista, M. Pedrosa, F. Curate, M.T. Ferreira, M.P.M. Marques, Estimation of the post-  
403 mortem interval in human bones by infrared spectroscopy, *Int. J. Legal Med.* 136(1) (2022)  
404 309-317.

405 [17] P.S. Garagoda Arachchige, J.L. Hughes, L.S. Bell, K.C. Gordon, S.J. Fraser - Miller,  
406 Detection of structural degradation of porcine bone in different marine environments with  
407 Raman spectroscopy combined with chemometrics, *J. Raman Spectrosc.* (2021).  
408 [18] L. Ortiz-Herrero, B. Uribe, L.H. Armas, M.L. Alonso, A. Sarmiento, J. Irurita, R.M. Alonso,  
409 M.I. Maguregui, F. Etxeberria, L. Bartolome, Estimation of the post-mortem interval of human  
410 skeletal remains using Raman spectroscopy and chemometrics, *Forensic Sci. Int.* 329 (2021)  
411 111087.  
412 [19] C. Bertinetto, J. Engel, J. Jansen, ANOVA simultaneous component analysis: A tutorial  
413 review, *Anal Chim Acta X* 6 (2020) 100061.  
414 [20] K. Zhang, F. Fan, M. Tu, J.-H. Cui, J.-S. Li, Z. Peng, Z.-H. Deng, The role of multislice  
415 computed tomography of the costal cartilage in adult age estimation, *Int. J. Legal Med.* 132(3)  
416 (2018) 791-798.  
417 [21] M. Partido Navadijo, I. Fombuena Zapata, E.A. Borja Miranda, I. Alemán Aguilera,  
418 Discriminant functions for sex estimation using the rib necks in a Spanish population, *Int. J.*  
419 *Legal Med.* 135(3) (2021) 1055-1065.  
420 [22] T. Pascart, B. Cortet, C. Olejnik, J. Paccou, H. Migaud, A. Cotten, Y. Delannoy, A. During, P.  
421 Hardouin, G. Penel, G. Falgayrac, Bone Samples Extracted from Embalmed Subjects Are Not  
422 Appropriate for the Assessment of Bone Quality at the Molecular Level Using Raman  
423 Spectroscopy, *Anal. Chem.* 88(5) (2016) 2777-83.  
424 [23] R.E. Adlam, T. Simmons, The effect of repeated physical disturbance on soft tissue  
425 decomposition--are taphonomic studies an accurate reflection of decomposition?, *J. Forensic*  
426 *Sci.* 52(5) (2007) 1007-14.  
427 [24] G. Falgayrac, B. Cortet, O. Devos, J. Barbillat, V. Pansini, A. Cotten, G. Pasquier, H. Migaud,  
428 G. Penel, Comparison of two-dimensional fast Raman imaging versus point-by-point  
429 acquisition mode for human bone characterization, *Anal. Chem.* 84(21) (2012) 9116-23.  
430 [25] J.J. Jansen, H.C.J. Hoefsloot, J. Van Der Greef, M.E. Timmerman, J.A. Westerhuis, A.K.  
431 Smilde, ASCA: analysis of multivariate data obtained from an experimental design, *Journal of*  
432 *Chemometrics* 19(9) (2005) 469-481.  
433 [26] A.K. Smilde, J.J. Jansen, H.C.J. Hoefsloot, R.-J.A.N. Lamers, J. Van Der Greef, M.E.  
434 Timmerman, ANOVA-simultaneous component analysis (ASCA): a new tool for analyzing  
435 designed metabolomics data, *Bioinformatics* 21(13) (2005) 3043-3048.  
436 [27] M. Anderson, C.T. Braak, Permutation tests for multi-factorial analysis of variance, *Journal*  
437 *of Statistical Computation and Simulation* 73(2) (2003) 85-113.  
438 [28] D.J. Vis, J.A. Westerhuis, A.K. Smilde, J. Van Der Greef, Statistical validation of megavariate  
439 effects in ASCA, *BMC Bioinformatics* 8(1) (2007) 322.  
440 [29] J. Camacho, C. Díaz, P. Sánchez - Rovira, Permutation tests for ASCA in multivariate  
441 longitudinal intervention studies, *Journal of Chemometrics* (2022).  
442 [30] H. Schielzeth, S. Nakagawa, Nested by design: model fitting and interpretation in a mixed  
443 model era, *Methods Ecol. Evol.* 4(1) (2013) 14-24.  
444 [31] T.S. Madssen, G.F. Giskeodegard, A.K. Smilde, J.A. Westerhuis, Repeated measures ASCA+  
445 for analysis of longitudinal intervention studies with multivariate outcome data, *PLoS Comput.*  
446 *Biol.* 17(11) (2021) e1009585.  
447 [32] G. Zwanenburg, H.C.J. Hoefsloot, J.A. Westerhuis, J.J. Jansen, A.K. Smilde, ANOVA-  
448 principal component analysis and ANOVA-simultaneous component analysis: a comparison,  
449 *Journal of Chemometrics* 25(10) (2011) 561-567.

450 [33] M. Bevilacqua, R. Bucci, S. Materazzi, F. Marini, Application of near infrared (NIR)  
451 spectroscopy coupled to chemometrics for dried egg-pasta characterization and egg content  
452 quantification, *Food Chem.* 140(4) (2013) 726-34.

453 [34] P. Firmani, R. Vitale, C. Ruckebusch, F. Marini, ANOVA-Simultaneous Component analysis  
454 modelling of low-level-fused spectroscopic data: A food chemistry case-study, *Anal. Chim.*  
455 *Acta* 1125 (2020) 308-314.

456 [35] S. De Luca, M. De Filippis, R. Bucci, A.D. Magrì, A.L. Magrì, F. Marini, Characterization of  
457 the effects of different roasting conditions on coffee samples of different geographical origins  
458 by HPLC-DAD, NIR and chemometrics, *Microchem. J.* 129 (2016) 348-361.

459 [36] A. Amadasi, A. Cappella, C. Cattaneo, P. Cofrancesco, L. Cucca, D. Merli, C. Milanese, A.  
460 Pinto, A. Profumo, V. Scarpulla, E. Sguazza, Determination of the post mortem interval in  
461 skeletal remains by the comparative use of different physico-chemical methods: Are they  
462 reliable as an alternative to (14)C?, *Homo* 68(3) (2017) 213-221.

463 [37] S. Longato, C. Wöss, P. Hatzler-Grubwieser, C. Bauer, W. Parson, S.H. Unterberger, V.  
464 Kuhn, N. Pemberger, A.K. Pallua, W. Recheis, R. Lackner, R. Stalder, J.D. Pallua, Post-mortem  
465 interval estimation of human skeletal remains by micro-computed tomography, mid-infrared  
466 microscopic imaging and energy dispersive X-ray mapping, *Analytical Methods* 7(7) (2015)  
467 2917-2927.

468 [38] M.P.M. Marques, A.P. Mamede, A.R. Vassalo, C. Makhoul, E. Cunha, D. Goncalves, S.F.  
469 Parker, L.A.E. Batista de Carvalho, Heat-induced Bone Diagenesis Probed by Vibrational  
470 Spectroscopy, *Sci. Rep.* 8(1) (2018) 15935.

471 [39] N. Kourkoumelis, M. Tzaphlidou, Spectroscopic Assessment of Normal Cortical Bone:  
472 Differences in Relation to Bone Site and Sex, *The Scientific World JOURNAL* 10 (2010) 402-412.

473 [40] J.S. Yerramshetty, C. Lind, O. Akkus, The compositional and physicochemical homogeneity  
474 of male femoral cortex increases after the sixth decade, *Bone* 39(6) (2006) 1236-43.

475 [41] M.D. Grynypas, R.G. Hancock, C. Greenwood, J. Turnquist, M.J. Kessler, The effects of diet,  
476 age, and sex on the mineral content of primate bones, *Calcif. Tissue Int.* 52(5) (1993) 399-405.

477 [42] G. Falgayrac, D. Farlay, C. Poncon, H. Behal, M. Gardegaront, P. Ammann, G. Boivin, B.  
478 Cortet, Bone matrix quality in paired iliac bone biopsies from postmenopausal women treated  
479 for 12 months with strontium ranelate or alendronate, *Bone* 153 (2021) 116107.

480 [43] G.S. Mandair, M.P. Akhter, F.W.L. Esmonde-White, J.M. Lappe, S.P. Bare, W.R. Lloyd, J.P.  
481 Long, J. Lopez, K.M. Kozloff, R.R. Recker, M.D. Morris, Altered collagen chemical compositional  
482 structure in osteopenic women with past fractures: A case-control Raman spectroscopic  
483 study, *Bone* 148 (2021) 115962.

484 [44] C.M. Weaver, K.M.H. Gallant, Chapter 14 - Nutrition, in: D.B.B.R. Allen (Ed.), *Basic and*  
485 *Applied Bone Biology*, Academic Press, San Diego, 2014, pp. 283-297.

486 [45] Y.N. Yeni, J. Yerramshetty, O. Akkus, C. Pechey, C.M. Les, Effect of fixation and embedding  
487 on Raman spectroscopic analysis of bone tissue, *Calcif. Tissue Int.* 78(6) (2006) 363-71.

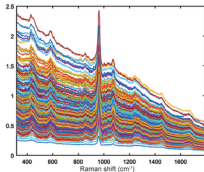
488

## RAMAN ANALYSIS OF SKELETAL REMAINS

Intrinsic and extrinsic factors



Influence of each factor is mixed in all Raman spectra (X)



## ANOVA-SIMULTANEOUS COMPONENT ANALYSIS

$$X = X_A + X_B + X_{AB} + E$$

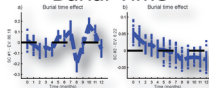
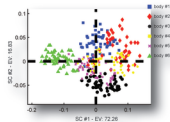


Unmix and separate  
intrinsic and extrinsic factors

## RANKING INTRINSIC AND EXTRINSIC FACTORS

15.66%  
Burial Time

7.54%  
Body source



2

1